A comparison of satellite-derived sea-ice motion with drifting-buoy data in the Weddell Sea

Sandra SCHWEGMANN,[1] Christian HAAS,[2] Charles FOWLER,[3] Rüdiger GERDES[1]

[1]Alfred Wegener Institute for Polar and Marine Research, Bremerhaven, Germany[**AUTHOR: please provide fuller address details for all authors**]
E-mail: Sandra.Schwegmann@awi.de
[2]University of Alberta, Edmonton, Canada
[3]Colorado Center for Astrodynamics Research, University of Colorado at Boulder, USA

ABSTRACT. We compare a satellite-derived sea-ice motion dataset obtained from the US National Snow and Ice Data Center (NSIDC) with daily ice drift by drifting buoys between 1989 and 2005. The satellite data were derived from daily composites of passive-microwave satellite measurements by means of a cross-correlation method and were supplemented with data from visible and thermal channels of the Advanced Very High Resolution Radiometer (AVHRR). Seasonal and interannual variations of the agreement between both datasets are discussed. In addition, regional differences in the agreement and correlation coefficients of buoy- and satellite-derived drift components have been analyzed. Results show that the overall drift regime can be well described by satellite-derived drift data but 71% of the retrieved drift velocities are lower than those observed by buoys. Nevertheless, correlation coefficients (r) between both datasets are 0.587 for the zonal and 0.613 for the meridional drift component. The correlation coefficients between monthly averages of buoy- and satellite-derived zonal and meridional drift components are on average 25.7% and 16.4% lower in summer (October–February) than in winter (March–September), with the exception of January. In January, correlation coefficients are about 62.6% (zonal) and 66.5% (meridional) lower than in winter. Furthermore, deviations between zonal buoy- and satellite-derived drift are 80% larger in the second half (July–December) than in the first half of the year. The observed yearly and regional averaged agreement between both datasets depends strongly on the season when buoy data were collected and on the number of coincident buoy and satellite data, which was often very low.

INTRODUCTION

Sea-ice drift modifies the heat exchange between ocean and atmosphere as well as ice export and consequently freshwater fluxes. Furthermore, the transport of latent heat is highly related to ice advection, since it influences the oceanic density structure due to salt release in regions of strong ice formation and freshening in regions of strong ice melting. This process is very important in the Weddell Sea (Harder and Fischer, 1999).

A further special feature of the Weddell Sea is that ice drift is influenced by the Antarctic Peninsula, resulting in high deformation and preventing in- and outflow of ice from and into the Bellingshausen Sea. This constriction of sea-ice drift influences the ice-thickness distribution, leading to thick strongly deformed ice in the southwestern part of the Weddell Sea, which can survive a summer period and becomes second-year ice (SYI). This SYI is transported from the southwestern region to the north, contributing to a high freshwater volume flux. The largest area of SYI in the Southern Ocean exists in the Weddell Sea. Furthermore, the Weddell Sea has the largest ice extent in winter, up to 2200 km from the coast (Harms and others, 2001), influencing the energy budget of the ocean and the atmosphere. All in all, ice drift modifies albedo, ocean stratification and deformation processes in the Southern Ocean, which are of high importance, particularly in the Weddell Sea. Therefore, for an understanding of the interaction of these effects, adequate knowledge of sea-ice drift and the errors of datasets are important.

Despite this need, there are only few sea-ice drift datasets available. Ice drift with high accuracy and high temporal and spatial resolution is provided by drifting-buoy data. With these data, regional studies can be performed, as well as an observation of the general large-scale drift behavior in regions covered by drifting buoys. However, due to logistic constraints and an irregularly distributed number of deployed buoys, this dataset does not cover the sea-ice zone sufficiently to study long-term characteristics of sea-ice drift or sea-ice export and accordingly freshwater fluxes. For such studies, ice drift derived from satellite data, and also model results, would be much more appropriate because of their large-scale and regular coverage.

In the present study, satellite-derived ice-drift data are compared with drifting-buoy data from 1989 to 2005 to assess the agreement between both datasets. A similar study was conducted by Schmitt (2005) for satellite-derived ice drift obtained from an optimally interpolated combination of measurements from the Scanning Multichannel Microwave Radiometer (SMMR) and Special Sensor Microwave Imager (SSM/I) 37 GHz and 85 GHz channels, which are combined with buoy data and interpolated onto a grid with 100 km spatial resolution. Schmitt compared this merged drift product, the so-called SSMI Optimal Interpolated Data (OI; http://imkhp7.physik.uni-karlsruhe.de/~eisatlas), with buoy data for the months March–November until 1997 and found that the overall drift velocities of the OI data are lower than the drift velocities obtained by buoys with a total mean root-mean-square error of 4.96 cm s^{-1} and a bias of –

2.62 cm s^{-1} (Schmitt, 2005) for the entire Antarctic sea-ice region. Compared with that former study, the dataset used here is extended by Advanced Very High Resolution Radiometer (AVHHR) data, includes data from the austral summer (December–February) and extends the comparison period until 2005, the year from which the last buoy data are available for the Weddell Sea. However, in the present study we compare a pure satellite product that has a spatial resolution of 25 km with buoy-derived ice-drift data. Therefore, this satellite product is independent of the buoy data used for this comparison.

Recently Heil and others (2001) compared buoy- and satellite-derived sea-ice motion in East Antarctica. In their study, drift trajectories from buoys were compared with corresponding drift trajectories from satellite-derived ice-motion vectors for different subregions and the entire East Antarctic sea-ice zone. The study found that broad-scale ice-drift patterns observed by buoys can be reproduced by satellite-derived data but also that ice-motion velocities from satellites are too low (Heil and others, 2001). This raises the question as to whether the satellite-derived sea-ice drift product shows a similar behavior in the Weddell Sea or is different due to the occurrence of a high amount of SYI and the drift restriction by the Antarctic Peninsula.

DATA DESCRIPTION

Satellite-derived data

Satellite-derived Polar Pathfinder sea-ice motion vectors, a merged product of drift vectors from SMMR (1978–1987), SSM/I (1987–2006) and AVHRR (1981–2000) images (http://nsidc.org/data/nsidc-0116.html) are provided by the US National Snow and Ice Data Center (NSIDC). Drift velocities are obtained by a maximum cross-correlation method, using daily composites of brightness temperature fields from the vertical and horizontal polarization of both the 37 GHz (SMMR and SSM/I) and the 85.5 GHz channels (SSM/I), as well as signals of the visible and thermal channels of AVHHR data, to calculate displacement vectors for special patterns, which have high correlation between sequential days (e.g. Ninnis and others, 1986; Emery and others, 1991).

The derived drift vectors of each sensor are merged by an optimal interpolation method for all areas where ice concentration exceeds 50% (Fowler and others, 2001). This method results in ice-drift fields without gaps. Data are provided with a daily resolution and have a spatial resolution of 25 km, showing the mean large-scale displacement vectors on a regularly spaced grid from November 1978 until December 2006. The drift vectors are georeferenced to an azimuthal equal area projection and positions are given in grid coordinates. In contrast to the Arctic sea-ice motion product, these Antarctic sea-ice motion fields do not include buoy data and therefore this product is independent of those used for the comparisons made in this study.

The advantage of the Eulerian drift fields is the large-scale coverage. However, temporal and spatial resolutions are limited to a resolution of 25 km for the 37 GHz channel and about 12.5 km for the 85.5 GHz channel. In addition, composed brightness temperatures for 1 day are obtained from overpasses of different times and also different locations per day, which could smear or blur the brightness temperature fields (Kwok and others, 1998). A further problem is the sensitivity to high water content in the

atmosphere of the 85.5 GHz channel. Under unfavorable conditions, this could lead to an interpolation of only a few drift vectors onto large areas of the grid and therefore to an overrepresentation of the interpolated drift regime.

The AVHRR has a higher temporal and spatial resolution. Up to four passes are used for daily composites, when available. In addition, AVHRR has a wide swath (>1000 km) and a high resolution of about 1 km. Unfortunately, this sensor is highly sensitive to clouds and atmospheric water vapor (http://nsidc.org/data/nsidc-0116.html; Heil and others 2001); therefore, data are only available for days with clear-sky conditions, resulting in many data gaps and probably in an underrepresentation of ice-drift regimes under any less favorable weather conditions. For more information on the merged sea-ice drift dataset see http://nsidc.org/data/nsidc-0116.html.

Drifting-buoy data

Polar Pathfinder sea-ice motion vectors were compared with vectors obtained from drifting buoys deployed on ice floes. The positions of those buoys were usually observed several times per day and were transmitted to the Argos satellite communication system. Two different types of position data are available. Earlier buoys were located by the Argos system using Doppler range finding (Heil and others, 2001). The accuracy of these positions is approximately 0.5 km (Emery and others, 1997; Harder and Fischer, 1999). Since 1997, newer buoys have included GPS receivers, which results in position accuracies of better than 50 m (Heil and others, 2001). Using the position data, drift vectors were derived and have been projected onto a regular hourly time grid, with the exception of the data since 2001, which were provided as 3 hourly position records. To allow for a comparison with the satellite-derived ice motions, which were derived from changes in daily composites of image patterns of sequential days, the hourly spaced buoy drift vector components were averaged into daily mean values using the data from 0000 h to 2400 h every day, centered on 1200 h.

The buoy ice-drift dataset provides Lagrangian drift trajectories with high spatial and temporal resolution as well as high accuracy but with limited spatial and temporal coverage. The spatial distribution of the buoy data, available for the years 1989–1999 and 2001, 2002, 2004 and 2005, is shown in Figure 1, with initial positions of all buoys used for this study. The number of buoys deployed varied between maximum values of 15 in 1989, 13 in 1992 and 11 in 1996/97 to a minimum of three buoys in 2004/05 and only one buoy in December of 2001. Data are obtained from various sources. Most data are provided by the Alfred Wegener Institute, available on the Pangaea website**[AUTHOR: is it appropriate to provide details of the website?]**. Some other buoy data were provided by the International Programme for Antarctic Buoys.

Data processing

For a comparison between both datasets, a bilinear interpolation of the daily mean satellite-derived zonal and meridional ice-drift components onto the daily mean buoy positions has been performed. Interpolation was done only when all velocities from surrounding gridpoints were available. Consequently, some data near the ice edge had to be excluded and quality analysis is not included for this region.
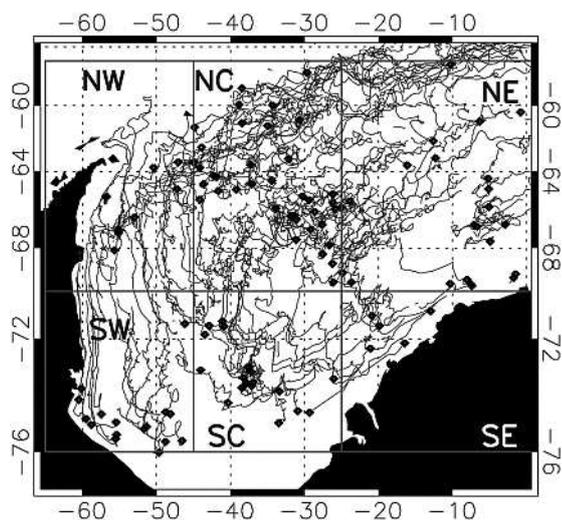
Fig. 1. Distribution of buoy start positions between 1989 and 2005 (symbols) and their drift tracks (gray lines). See Table 1 for region abbreviations.

Owing to the fact that the satellite-derived drift vectors are given in grid coordinates, they had to be rotated based upon their longitude to get the zonal (east–west) and meridional (north–south) drift components at the daily mean buoy positions. Afterwards, differences for both drift components were calculated by subtracting the satellite-derived from the daily mean buoy-derived ice drift ($u/v\,B - u/v\,S$). Statistical significance of differences and correlation coefficients were proved by using a Student's t test (e.g. Press and others, 2007).

In total, there are 11 928 coincident drift vector pairs for the entire study period. The number of data points that has been used for the calculation of yearly means varies strongly, depending on the number of buoys that were deployed in one particular year and the number of available satellite-derived ice-drift vectors for the buoy positions. For example, in 1990, 12 buoys were operated, but the number of corresponding drift vectors from both datasets is only $n = 58$. The reason for this difference is most likely the operating region (northern part, near ice edge) in conjunction with the season (beginning in January) of the respective buoys. The connections between regions, season and number of data points with the agreement between buoy- and satellite-derived ice drift will be reviewed in the discussion. The

maximum number of corresponding drift vectors in one particular year is 2010, obtained in 1996, when 11 buoys were deployed. Contrary to the yearly distribution, the number of monthly data points is relatively high and varies between the minimum of 440 data points in January up to a maximum of 1425 data points per month in October. In late spring, summer and early fall a higher number of buoy data are available than the number of coincident buoy- and satellite-derived vectors would suggest. This often occurred when buoys were located near the ice edge, especially when records were started in summer. A reasonable explanation is that satellite-derived ice drift was only calculated when ice concentration was higher than 50%. In addition, satellite-derived data close to the ice edge have been excluded from this study by the interpolation method. Therefore, some gaps can arise from the satellite-derived product for regions with lower ice concentrations where buoy-derived ice drift was still present. This would result in an earlier record of buoy-derived ice drift in fall and a longer record in spring compared with satellite-derived ice drift. An example is shown in Figure 2. This means that the number of coincident drift vectors is not only dependent on the number of deployed buoys but also on the ice concentration for which ice-drift vectors are calculated from satellites.

For an analysis of the different regions described in Table 1, n varies strongly with minimum values between 0 and 29 and a maximum of 688 in the northern central Weddell Sea. Hence, the number of corresponding data points contributing to mean values is highly dependent on the number of deployed buoys, the region and season of deployment and the ice concentration range used for satellite-derived ice-drift calculations.

RESULTS

Overall comparison

The daily mean buoy drift speed of all 11 928 data points was $0.135\,\mathrm{m\,s^{-1}}$, comparable with studies from Fischer (1995), Harder and Fischer (1999) and Kottmeier and Hartig (1990) who observed typical drift velocities of 0.10–$0.15\,\mathrm{m\,s^{-1}}$. The mean error of the buoy-derived daily ice drift is about $0.006\,\mathrm{m\,s^{-1}}$ for older buoys with location accuracy of approximately 0.5 km and $5.9 \times 10^{-4}\,\mathrm{m\,s^{-1}}$ for GPS drifters. The mean daily satellite-derived ice-drift velocity was $0.088\,\mathrm{m\,s^{-1}}$ for the same data points. This is 34.5% less than the mean buoy drift. The difference between both datasets is significantly different from zero at the 95%
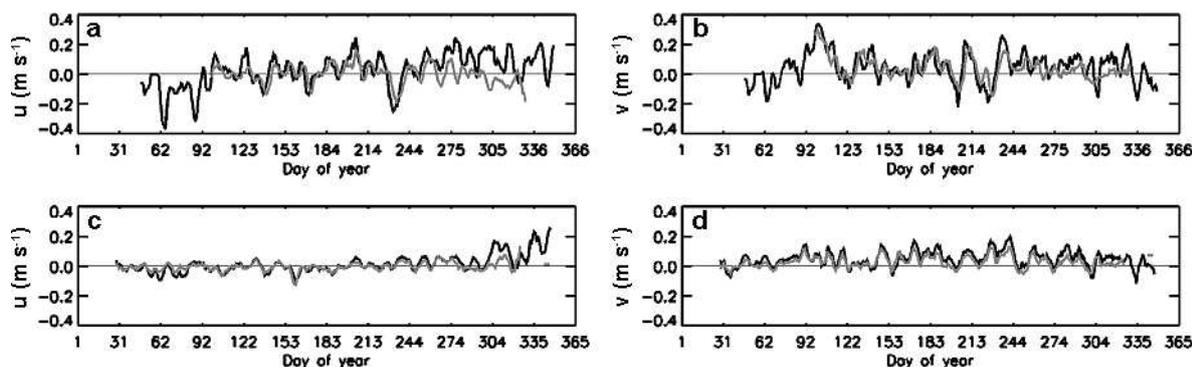
Fig. 2. 5 day running mean of buoy- (black) and satellite-derived (gray) (a,c) zonal and (b,d) meridional ice drift. Examples for a buoy in (a,b) 1996 and one in (c,d) 1999 are shown.

Table 1. Definition of different regions for local comparisons

Region	Longitude	Latitude
Northwest (NW)	65–45° W	57–70° S
Southwest (NW)	65–45° W	70–76° S
North-central (NC)	45–25° W	57–70° S
South-central (SC)	45–25° W	70–76° S
Northeast (NE)	25° W–10° E	57–70° S
Southeast (SE)	25° W–10° E	70–76° S

Fig. 4. Correlation between buoy data and satellite-derived drift for (a) the zonal (u) and (b) the meridional (v) component. Pairs of buoy and satellite drift vectors: 11 928. Time period: 1989–2005.

confidence interval. Of the satellite-derived ice-drift velocities, 71.1% are below those observed by buoys (not shown). This finding is similar to results from Heil and others (2001) who found that satellite-derived ice-drift speeds are generally lower those derived from buoys for the East Antarctic sea-ice zone. Only 10.85% of the satellite-derived drift velocities are within a range of ±10% of the buoy-derived drift velocities. Nevertheless, it also occurs that the velocities exceed those observed by buoys.

Figure 3 shows the distribution of differences between buoy- and satellite-derived ice drift for all data from 1989 to 2005 for the zonal u (east–west, positive in eastward direction) and meridional v (north–south, positive in northward direction) drift component. Mean buoy-derived drift components are $u = 0.012 \pm 0.112 \, \mathrm{m \, s^{-1}}$ and $v = 0.038 \pm 0.115 \, \mathrm{m \, s^{-1}}$. The mean satellite-derived drift is $u = 0.000 \pm 0.072 \, \mathrm{m \, s^{-1}}$ and $v = 0.027 \pm 0.079 \, \mathrm{m \, s^{-1}}$. The mean differences between both datasets, calculated by subtracting the satellite- from the buoy-derived drift, are significant at the 95% confidence interval with $\Delta u = 0.012 \pm 0.091 \, \mathrm{m \, s^{-1}}$ and $\Delta v = 0.010 \pm 0.091 \, \mathrm{m \, s^{-1}}$. Generally, differences of the meridional drift have a wider range than those of the zonal drift and the modal value for differences between buoy- and satellite-derived drift is $0.020 \, \mathrm{m \, s^{-1}}$ (Fig. 3). For the zonal drift, the range of differences is lower and the modal value is $-0.010 \, \mathrm{m \, s^{-1}}$. The absolute differences (buoy – satellite) are $0.062 \pm 0.067 \, \mathrm{m \, s^{-1}}$ for the zonal and $0.065 \pm 0.064 \, \mathrm{m \, s^{-1}}$ for the meridional drift. Correlation coefficients (r) between daily buoy- and satellite-derived data are 0.59 for the zonal and 0.61 for the meridional drift (Fig. 4).

Temporal and regional variability of differences between datasets

As buoys are unevenly distributed in time and space, data have been analyzed separately according to their temporal and regional distribution. In the beginning, all the data from 1 year are averaged into a yearly mean. In addition, data are averaged monthly for all years to study seasonal variations.

Figure 5 displays the yearly (Fig. 5a,b) and monthly (Fig. 5c,d) mean zonal (Fig. 5a,c) and meridional (Fig. 5b,d) drift speed, the averaged differences between both datasets and the number of data points that contribute to the mean values (n). Furthermore, the 95% confidence interval for the differences is added and indicates where mean differences are not significantly different from zero. The magnitude of both drift components shown in Figure 5 is generally too low for the satellite-derived sea-ice drift.

For the meridional drift component, the characteristics of the satellite-derived ice drift are comparable with those of the buoy-derived ice drift and deviations are lower than 50% in most years (not shown). In contrast, deviations between both datasets of the zonal drift component are often higher than 50% of the buoy-derived ice drift and, in some years, the satellite-derived component has the opposite direction of the buoy drift, for example in 1996 and 1998.

Correlation coefficients between daily drift velocity components derived from satellite data and from drifting buoys for single years, shown in Figure 6, vary between about 0.4 and 0.7 for both drift components. An exception was 1998, when correlation between buoy- and satellite-derived zonal drift was low and negative with a value of only –0.1, and low but positive at 0.34 for meridional drift. Furthermore, in 1990 and 2001, correlation coefficients between buoy- and satellite-derived meridional drift were only 0.24 and –0.25. The year 2001 even had a strong negative correlation for the meridional drift component. In those years, correlation coefficients are not significant at the 95% confidence interval. Possible reasons for this are given in the discussion.

Towards the end of the study period, absolute differences between buoy- and satellite-derived data decrease (not shown). For the zonal component, absolute deviations decrease by about $0.034 \, \mathrm{m \, s^{-1}}$ or 47% and by about $0.030 \, \mathrm{m \, s^{-1}}$ (41%) for the meridional drift during the study period. Additionally, the standard deviations of differences become smaller, suggesting that the more recent satellite-derived ice-drift data are of higher quality.

Fig. 3. Differences between buoy- and satellite-derived drift for (a) the zonal (u) and (b) the meridional (v) drift component. Bin size is $0.005 \, \mathrm{m \, s^{-1}}$. Pairs of buoy and satellite drift vectors: 11 928. Time period: 1989–2005.
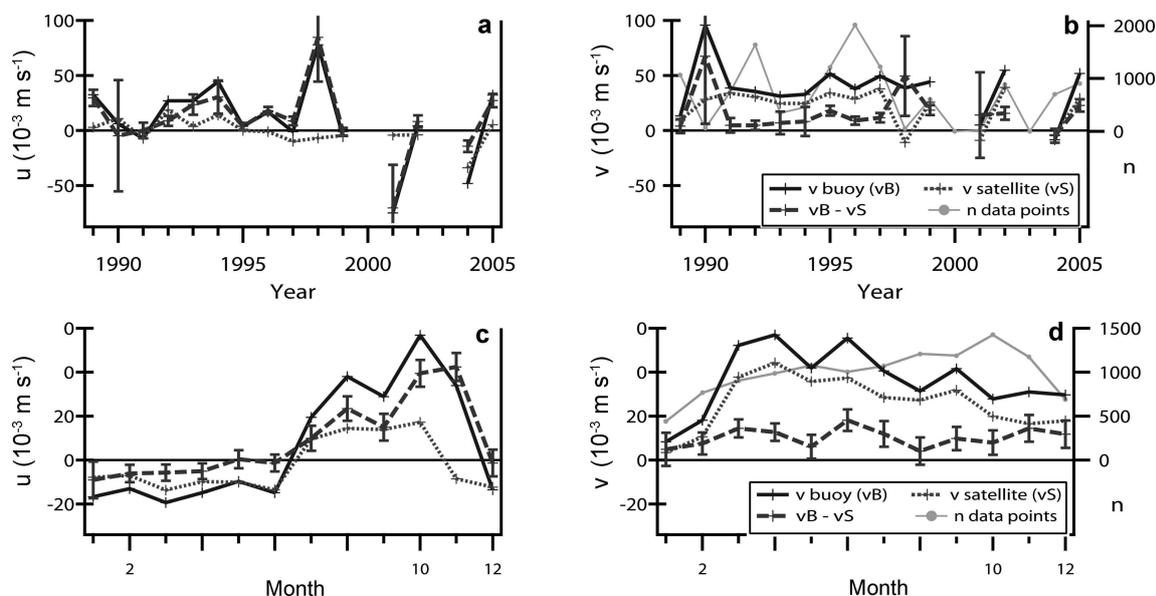
Fig. 5. Mean values for (a,c) zonal and (b,d) meridional components of buoy- (black) and satellite-derived (gray dotted line) drift, mean differences (gray, dashed line) with attached 95% confidence interval and number of corresponding drift vector pairs (*n*, light gray, only in (b) and (d)). (a,b) Yearly distribution and (c,d) monthly distribution are shown.

As yearly discrepancies and correlation coefficients of buoy- and satellite-derived drift show high variation from year to year and the buoys are not distributed regularly in time and space, an analysis of accuracies on a yearly basis cannot sufficiently explain which factor, either the temporal or the regional distribution, affects the accuracy of this particular satellite-derived dataset. Therefore, a seasonal as well as a regional study has been performed.

For the seasonal analysis, monthly averages were derived over the study period. Figure 5c shows that the mean prevailing zonal drift direction changes in July from westward (negative) to eastward (positive). The highest mean zonal drift speed of $0.057 \, \mathrm{m \, s^{-1}}$ (buoy) and $0.017 \, \mathrm{m \, s^{-1}}$ (satellite) was observed in October while the highest mean meridional drift speed of $0.057 \, \mathrm{m \, s^{-1}}$ (buoy) and $0.044 \, \mathrm{m \, s^{-1}}$ (satellite) occurs in April. Between July and November and also in January differences between zonal buoy- and satellite-derived ice drift exceed 50% of the respective buoy-derived zonal ice drift (Fig. 7). The differences of the meridional drift component, also shown in Figure 7, vary between 10 and 50% of the respective buoy-derived ice drift for all months, except in January. The lowest discrepancies, less than 33%, occur from March

through October. This means that the meridional drift component is somewhat more accurate from fall until mid-spring, while zonal drift discrepancies between buoy- and satellite-derived data start to increase in mid-winter (July; Figs 5 and 7) and are the highest in November (end of spring).

Correlation coefficients for the monthly separated daily mean drift velocities (Fig. 6b) vary little between 0.4 and 0.8, except in January when the correlation is about 0.2 for both the meridional and the zonal ice drift. All of them are statistically significant at the 95% confidence level. In most cases, the differences in correlation between buoy- and satellite-derived drift for zonal and meridional drift are <0.1. Mean summer correlations (October–February, without the January correlation) are about 26% (*u*) and 16% (*v*) lower than winter mean correlations (March–September). The correlation coefficient in January is only about 0.24 (*u*) and 0.22 (*v*) for the ice-drift components, and therefore 63.0% (for zonal) and 66.5% (for meridional drift) lower than winter mean correlations. The fact that the October–February correlations are somewhat lower than those for March–September and that differences between both datasets for both drift components are in general high from
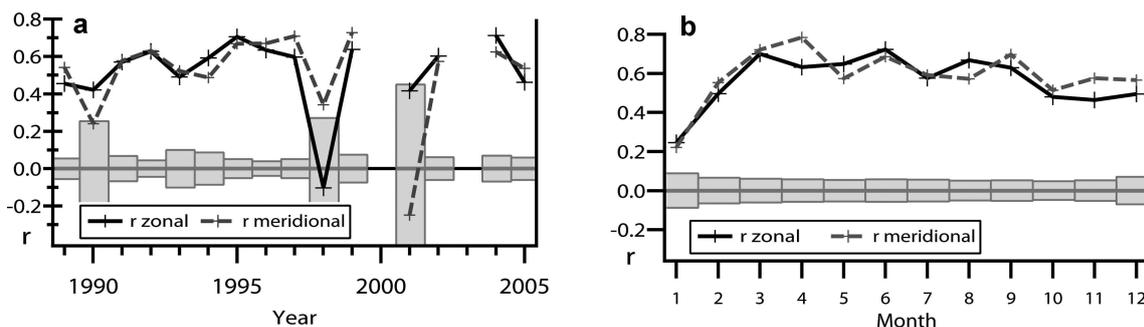
Fig. 6. Correlation (*r*) between zonal (black) and meridional (dark gray, dashed) components of buoy- and satellite-derived ice drift. (a) Yearly and (b) monthly distribution. Gray bars show the region of <95% confidence for the correlation coefficients being non-zero.
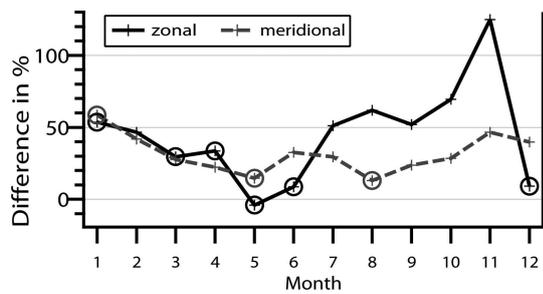
Fig. 7. Percentages of mean differences between buoy- and satellite-derived drift components (zonal–black, meridional–gray, dashed) for monthly distribution. Circles indicate that the confidence for differences being non-zero is <95% for each drift component.

October to February may be due to sudden emissivity changes resulting from snow wetting, as described by Willmes and others (2006, 2009), which can result in a loss of tracking features between sequential days. Furthermore, flooding events may change observed patterns from one day to another. These interactions may result in a reduction of satellite-derived ice-drift vectors and therefore in a wider interpolation of drift velocities.

Data have been separated into the six regions listed in Table 1 to study deviations between different regions.

Monthly variations of correlation coefficients for each region are shown in Figure 8. All regions have low correlation coefficients in January, which are mostly insignificant. This can be seen by the gray bars in Figure 8, which show the region of <95% confidence for the correlation coefficients. Where the data points lie in between these gray bars, results are not significant. In all other months, correlation coefficients show higher variations between about 0.4 and 0.8, which is comparable with the correlation coefficients obtained for the entire Weddell Sea shown in Figure 6. It is remarkable that the same declining behavior is seen for the north-central and northeast part where correlation coefficients start to decrease slightly in early spring, which could be a result of surface melt. For the eastern part of the Weddell Sea, mean correlation is below 0.5 for both drift components in the southern part, while other regions have a mean correlation coefficient higher than 0.5. The September correlation of the meridional component is even negative in the southeastern Weddell Sea, but is statistically insignificant at the 95% confidence level. Again, there seems to be a relation with the number of corresponding data points contributing to the correlation calculation, which was only 16 for September in the southeast region. However, the low mean correlation for the southeastern Weddell Sea is a result of the low September correlation of 0.04 (u) and –0.1 (v). Excluding these values, the mean correlation from January through August is above 0.5. Furthermore, the averaged September vectors are all obtained in just 1 year, namely
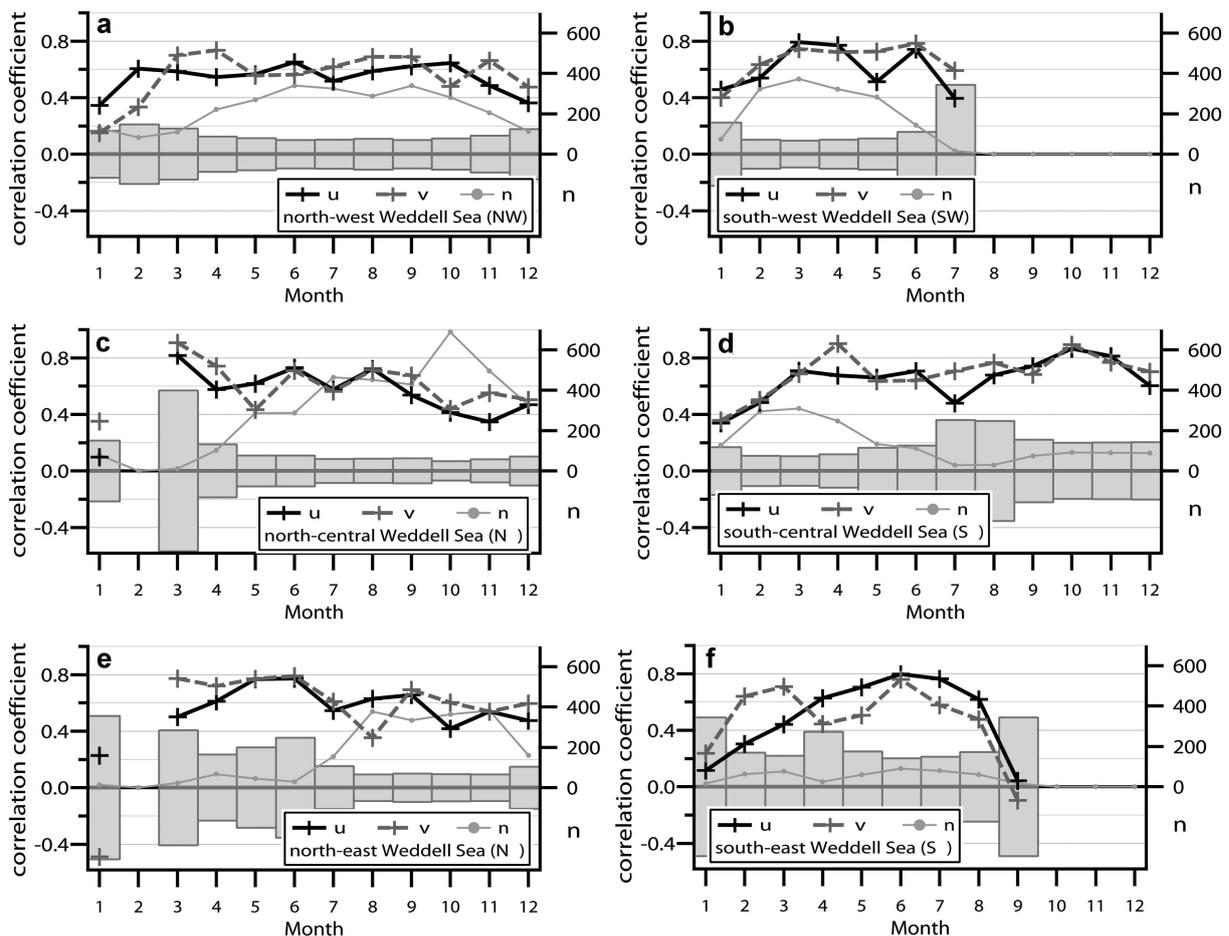
Fig. 8. Correlation between zonal (black) and meridional (dark gray, dashed) components of buoy- and satellite-derived ice drift for monthly separated data and number of corresponding drift vector pairs n (light gray) for different regions. Gray bars show the region of <95% confidence for the correlation coefficients being non-zero.

2004. Therefore, this value represents only one month and not a long-term monthly mean and cannot be compared with other correlation coefficients in the same way that the long-term means are compared. Finally it seems that the correlation coefficients do not significantly vary between different regions in the Weddell Sea.

DISCUSSION

The comparison between buoy- and satellite-derived ice drift shows that agreements between both datasets depend on the averaging method. Comparing the yearly averages, correlation coefficients (Fig. 6) and deviations (Fig. 5) differ strongly in the years 1990, 1998 and 2001 from the general correlation coefficients of 0.4 up to 0.8 in other years. What these years have in common is that the number of corresponding data points contributing to the yearly averages is very low, only 19–58. In 1990 and 1998, most data were collected in January, which shows the overall lowest correlation between both datasets (Fig. 6b). However, this explanation cannot be used for 2001, when data were collected in December. In this year, the region (northeast) and especially the low value for n (19) seem to be the main reasons for the low and negative correlation of –0.25 for the meridional drift and the high difference of 94% between buoy- and satellite-derived zonal drift. In those years, it is possible that single extreme events strongly influenced the comparison due to the low number of comparable vectors, since buoys can capture these extreme events and the compared satellite-derived drift may not, for example due to the interpolation of drift vectors from a region or a point in time with more favorable weather conditions for detecting changes in signal features. In addition, signals can be influenced by inaccuracies of the satellite-derived ice-drift vectors near the ice edge, since most of the data in 1990, 1998 and 2001 were collected in the northern parts of the Weddell Sea, near the ice edge. The fact that the correlation coefficients are not significant at the 95% confidence level supports the position that the correlations of the respective drift component for those years may not be reliable.

Since buoy data do not cover the Weddell Sea regularly in time and space, a reliable study of the interannual behavior does not seem to be possible. However, to analyze the dependency of the agreement between buoy- and satellite-derived ice drift on seasons, monthly averages were derived over the study period. The highest discrepancies for the mean zonal drift occur from July through November, while correlations do not show extraordinarily low values for the entire Weddell Sea for this period. This highlights the importance of the considered season. From July through November, buoy-derived zonal drift is on average 2.5 times higher than ice drift from December to June. As mentioned before, the Polar Pathfinder satellite-derived drift velocities are most often too low and the highest differences of the zonal drift component occur between July and November. This can arise because clusters of pixels from daily composites of satellite images from one day to the next are correlated to obtain drift velocities, resulting in averaging signals observed at different times and locations over large areas each day, which could lead to a drift-speed-dependent blurring or smearing of the brightness temperature fields (Kwok and others, 1998), while daily mean buoy data describe accurate small-scale drift features from in situ Lagrangian tracks. In addition, ridging and rafting, as well as

rotation, cause changes in signal features and can lead to failure of the tracking of high ice motion (Heil and others, 2001). Finally, the interpolation onto the regularly spaced grid also influences mean ice drift, especially when only a few velocity vectors are available for a large region. Therefore, the detection of high drift speeds is difficult and may be underrepresented in the satellite data. Hence, differences between buoy- and satellite-derived ice drift become higher when drift velocities increase, as results from July through November indicate. Another factor is that drift velocities can be derived only via cross-correlation when the distribution of signal patterns does not change very strongly over short time periods, for example due to changing snow properties, ice concentrations or flooding (Willmes and others, 2009). This seems to be the reason for the lower correlation coefficients from October to March, especially in January, and is also a strong indicator for the seasonal dependency of agreements between buoy- and satellite-derived ice drift. Furthermore, this could be an explanation for the extremely high differences for the zonal drift component in November, where both the general high drift velocities and surface changes may influence the results.

Differences between both datasets might be reduced when using orbital data instead of daily means, since information about observation time and location does not appear in an averaged dataset, as Kwok and others (1998) already stated.

An analysis of the regional effects on the agreement between both datasets indicates that there are regional differences, but these are not very large. It seems that the season as well as the number of corresponding vectors influences the agreement between buoy and the satellite vectors more than the region.

The study results indicate that the general drift behavior, captured by a high number of buoys on single ice floes, can be described by this satellite product as long as the satellite-derived drift is used for large-scale drift pattern and is averaged for longer time periods, for example over 1 month. Daily buoy-derived means can include some extreme events which cannot be derived accurately enough by this satellite product due to the large-scale averaging of drift speeds from different regions and times per day. Hence, comparisons of these single days would lead to a high discrepancy between both datasets. By averaging buoy- as well as satellite-derived ice drift for longer time periods, the extreme events might be smoothed out and a comparison would lead to lower discrepancies.

CONCLUSIONS

A comparison of buoy- and satellite-derived ice-drift data between 1989 and 2005 shows that the mean satellite-derived Polar Pathfinder sea-ice drift underestimates the mean drift velocity of drifting buoys by 34.5%, but the general drift pattern in the Weddell Sea can be described by this product. However, fast ice-drift events and ice concentrations below 50%, as well as special regions like coasts or the ice edge, can result in a loss of tracking features and therefore lead to high differences between buoy- and satellite-derived ice drift because of the interpolation of ice-drift vectors in these satellite data. Differences between both datasets are the highest from July through November for the zonal drift component. Except in January, correlation coefficients are similar for the entire Weddell Sea in all

months but are slightly higher in winter. This finding supports partly the results from Emery and others (1997), who state that winter sea-ice motion fields are most likely the more accurate ones. On the other hand, the high differences between both datasets in winter contradict this statement. The influence of different regions on the agreement between both datasets is less important than seasonal effects, except for regions near the ice edge. Unfortunately, the question as to whether the Polar Pathfinder satellite-derived sea-ice motion product for the Weddell Sea shows a behavior similar to that in the study of Heil and others (2001), or whether it is different due to the occurrence of a high amount of SYI and the drift restriction by the Antarctic Peninsula, cannot be answered in detail by this study. More than two-thirds of the drift velocities are too low, which is similar to the results for the East Antarctic ice zone by Heil and others (2001), who found that drift velocities are generally too low for the satellite product they used. However, regional behavior does not vary as strongly as was found for the East Antarctic ice zone and the influence of either the SYI or the Antarctic Peninsula cannot be clearly indicated due to the sparse coverage of buoy data in the Weddell Sea.

Finally, the general ability of this particular satellite-derived sea-ice drift product to represent the general ice circulation pattern makes it possible to use these data for large-scale and long-term analysis of drift behavior, if it is taken into account that the mean drift velocity is about one-third too low compared with the mean drift velocity obtained by sea-ice buoy trajectories. For ice and freshwater flux experiments these data should be used carefully. Monthly means may be more adequate for such studies, because daily drift vectors can differ strongly from in situ data (see deviations in Fig. 3), not only with regard to drift velocity but also in drift direction. Furthermore, it is questionable as to whether an analysis of deformation processes can be conducted with this particular satellite-derived ice-motion product. Not only the fact that ice drift cannot be detected in zones of high deformation (http://nsidc.org/data/nsidc-0116.html), due to structure loss, but also eventually inaccurate ice directions and displacements, which are too small, may lead to an underestimation of deformation processes. Other satellite data with a higher resolution might be more useful for these kinds of studies. Nevertheless, a comparison of buoy-derived deformation parameters with this particular satellite product is currently underway.

REFERENCES

Emery, W.J., C.W. Fowler, J. Hawkins and R.H. Preller. 1991. Fram Strait satellite image-derived ice motions. *J. Geophys. Res.,* **96**(C3), 4751–4768.

Emery, W.J., C.W. Fowler and J.A. Maslanik. 1997. Satellite-derived maps of Arctic and Antarctic sea-ice motion. *Geophys. Res. Lett.,* **24**(8), 897–900.

Fischer, H. 1995. Vergleichende Untersuchungen eines optimierten dynamisch-thermodynamischen Meereismodells mit Beobach-tungen im Weddellmeer. *Ber. Polarforsch.,* **166**.

Fowler, C.W., W.J. Emery and J.A. Maslanik. 2001. Twenty three years of Antarctic sea ice motion from microwave satellite imagery. *In Proceedings of International Geoscience and Remote Sensing Symposium (IGARSS 2001), 9–13 July 2001.* Piscataway, NJ, Institute of Electrical and Electronics Engineers, 157–159..

Harder, M. and H. Fischer. 1999. Sea ice dynamics in the Weddell Sea simulated with an optimized model. *J. Geophys. Res.,* **104**(C5), 11,151–11,162.

Harms, S., E. Fahrbach and V.H. Strass. 2001. Sea ice transport in the Weddell Sea. *J. Geophys. Res.,* **106**(C5), 9057–9073.

Heil, P., C.W. Fowler, J.A. Maslanik, W.J. Emery and I. Allison. 2001. A comparison of East Antarctic sea-ice motion derived using drifting buoys and remote sensing. *Ann. Glaciol.,* **33**, 139–144.

Kottmeier, C. and R. Hartig. 1990. Winter observations of the atmosphere over Antarctic sea ice. *J. Geophys. Res.,* **95**(D10), 16,551–16,560.

Kwok, R., A. Schweiger, D.A. Rothrock, S. Pang and C. Kottmeier. 1998. Sea ice motion from satellite passive microwave imagery assessed with ERS SAR and buoy motions. *J. Geophys. Res.,* **103**(C4), 8191–8214.

Ninnis, R.M., W.J. Emery and M.J. Collins. 1986. Automated extraction of pack ice motion from advanced very high resolution radiometer imagery. *J. Geophys. Res.,* **91**(C9), 10,725–10,734.

Press, W.H., S.A. Teukolsky, W.T. Vetterling and B.P. Flannery. 2007. *Numerical recipes: the art of scientific computing.* Third edition. Cambridge, etc., Cambridge University Press, 727–730, 746.

Schmitt, C. 2005. Interannual variability in Antarctic sea ice motion. (PhD thesis, University of Karlsruhe.)

Willmes, S., J. Bareiss, C. Haas and M. Nicolaus. 2006. The importance of diurnal processes for the seasonal cycle of sea-ice microwave brightness temperatures during early summer in the Weddell Sea, Antarctica. *Ann. Glaciol.,* **44**, 297–302.

Willmes, S., C. Haas, M. Nicolaus and J. Bareiss. 2009. Satellite microwave observations of the interannual variability of snowmelt on sea ice in the Southern Ocean. *J. Geophys. Res.,* **114**(C3), C03006. (10.1029/2008JC004919.)